

Precipitation Pattern of the Mid-Holocene Simulated by a High-Resolution Regional Climate Model

YU Entao^{*1,2}, WANG Tao^{1,2}, GAO Yongqi^{1,3}, and XIANG Weiling⁴

¹*Nansen-Zhu International Research Centre, Institute of Atmospheric Physics, Chinese Academy of Sciences, Beijing, 100029*

²*Climate Change Research Center, Chinese Academy of Sciences, Beijing, 100029*

³*Nansen Environmental and Remote Sensing Center, Bergen, Norway, 5006*

⁴*State Key Laboratory of Atmospheric Boundary Layer Physics and Atmospheric Chemistry, Institute of Atmospheric Physics, Chinese Academy of Sciences, Beijing, 100029*

(Received 5 September 2013; revised 28 October 2013; accepted 7 November 2013)

ABSTRACT

Early proxy-based studies suggested that there potentially occurred a “southern drought/northern flood” (SDNF) over East China in the mid-Holocene (from roughly 7000 to 5000 years before present). In this study, we used both global and regional atmospheric circulation models to demonstrate that the SDNF—namely, the precipitation increases over North China and decreases over the lower reaches of the Yangtze River Valley—could have taken place in the mid-Holocene. We found that the SDNF in the mid-Holocene was likely caused by the lower SST in the Pacific. The lowered SST and the higher air temperature over mainland China increased the land–sea thermal contrast and, as a result, strengthened the East Asian summer monsoon and enhanced the precipitation over North China.

Key words: mid-Holocene, East China, southern drought/northern flood

Citation: Yu, E. T., T. Wang, Y. Q. Gao, and W. L. Xiang, 2014: Precipitation pattern of the mid-Holocene simulated by a high-resolution regional climate model. *Adv. Atmos. Sci.*, **31**(4), 962–971, doi: 10.1007/s00376-013-3178-9.

1. Introduction

East China is a major agricultural region with a dense population; its society and economy are quite vulnerable to the large variability in summer rainfall, which is connected to the East Asian summer monsoon (EASM) system. One of the most important features of summer rainfall over East China in recent years is the so-called decadal change/shift of “southern flood/northern drought” (Zhu et al., 2010); namely, the precipitation increases over South China and decreases over North China. This shift of precipitation pattern brings a new drought/flood pattern and large economic and environmental effects on East China, drawing much concern. The main factors influencing summer rainfall in East China, as identified by previous studies, include the East Asia summer monsoon (Wang, 2000a, 2001; Ding et al., 2008), the Tibetan Plateau (Zhao et al., 2010; Zhang et al., 2012), the North Atlantic Oscillation (Sun and Wang, 2012), the North Pacific Oscillation (Zhou and Xia, 2012), SST (Fu et al., 2009), El Niño Southern oscillation (ENSO) (Chang et al., 2000), and the Pacific Decadal Oscillation (PDO) (Zhu et al., 2010). Recent studies have found that the interannual variability of thermal

contrasts between East Asia and the Pacific, well indicated by the Asian–Pacific Oscillation (APO) index, exerts strong influences on changes in atmospheric circulation and rainfall over East Asia, and rainfall over East Asia often shows the southern drought/northern flood pattern corresponding to a strengthened thermal contrast (Zhao et al., 2007, 2011, 2012; Zhou and Zhao, 2010; Liu et al., 2011; Zhou et al., 2011).

What the main spatial pattern of summer rainfall over East China will be in the coming warmer world is another important issue. Projected results from simulations by models involved in phase 5 of the Coupled Model Intercomparison Project (CMIP5) indicate an overall wetter East China in summer (Chen et al., 2012; Zhang and Sun, 2012), with large uncertainties (Hawkins and Sutton, 2011; Knutti and Sedlacek, 2012). Along with future projections, paleoclimate studies provide another hint regarding precipitation change against a warm background, as well as the potential mechanism for understanding present and future climate change. By examining the response of climate models to forcings that are different from the present, paleoclimate simulations can also provide insight into potential future climate changes, as the main processes that shaped the climate in the past may also be important in the future (Diffenbaugh and Sloan, 2004).

One typical warm period drawing much attention is the mid-Holocene (from approximately 7000 to 5000 years be-

* Corresponding author: YU Entao
Email: yetsyu@mail.iap.ac.cn

fore present), in which time the incoming insolation altered with latitude and season due to a change in the Earth's orbital parameters (Berger, 1978; Kutzbach and Liu, 1997). Many numerical studies have been conducted to investigate if well-developed models (mainly global climate models) can reproduce the main climate change features of this period, and to explore the associated mechanism (Wang, 1999, 2000b, 2002; Otto-Bliesner et al., 2006; Braconnot et al., 2007; Brown et al., 2008; Hargreaves and Annan, 2009; Wang et al., 2010; Jiang et al., 2012; Wang and Wang, 2013). Proxy evidence indicates that North China was wetter (Wang et al., 2010), while the area that is now Shanghai (located in the lower reaches of the Yangtze River valley) would have been drier (Cai et al., 2001; Wang and Huang, 2006). This indicates that the rainfall pattern in the mid-Holocene was one of "southern drought/northern flood" (SDNF); namely, the precipitation increased over North China and decreased along the lower reaches of the Yangtze River valley. However, except for the study of Zhou and Xia (2012), which simulated well the southern drought/northern flood pattern in the mid-Holocene using CCSM3 (Community Climate System Model, version 3), most global climate models show an overall wetter condition over East China in the mid-Holocene (Wang, 2002; Wang et al., 2010), thus failing to reproduce the SDNF summer rainfall pattern. The reason for this model failure is still unclear.

It is well known that both large-scale and regional-scale climate processes shape climate at the regional scale. Previous studies have revealed that, for East China, where complex topography and the unique East Asian monsoon system are present (Wang, 2002; Chen et al., 2012), regional climate models (RCMs) can show improved performance over global climate models (Gao et al., 2006, 2011; Yu et al., 2010; Yu, 2013). Therefore, it is necessary to conduct regional-scale climate sensitivity studies to see whether high-resolution state-of-the-art RCMs can reproduce the SDNF summer rainfall pattern in East China against a warm background. In this study, we chose a newly-developed RCM, the Weather Research and Forecasting (WRF) model (Skamarock et al., 2008) with the Advanced Research WRF (ARW) core. In terms of the GCM for providing the initial and boundary conditions, we used a well-developed global climate model; namely, IAP (Institute of Atmospheric Physics)-AGCM (Atmospheric Global Climate Models), version 4 (IAP4) (Sun et al., 2012).

The remainder of the paper is structured as follows. Section 2 describes the models and datasets used, as well as results from verifying model performance. Section 3 presents

the main results of the model simulation and analyzes the underlying physical mechanisms. A discussion of the robustness and level of uncertainty in the simulation, as well as a summary of the key findings is presented in section 4.

2. Models and data

2.1. RCM and GCM models

The WRF model is a mesoscale numerical model, and is a popular atmospheric RCM under collaborative development by many organizations. The ARW consists of a model solver of fully compressible, Eulerian and nonhydrostatic equations with a run-time hydrostatic option. The model uses terrain-following, hydrostatic-pressure vertical coordinates, with the top of the model being a constant pressure surface. The horizontal grid is the Arakawa-C grid and the time integration scheme in the model uses the third-order Runge-Kutta scheme (Wicker and Skamarock, 2002). This model has been widely used in regional climate studies in East Asia (Yu et al., 2012; Ge et al., 2013; Yu, 2013), and the simulations indicate that the model has the ability to reproduce the main features of climate in this region.

IAP4 is a global atmospheric general circulation model, which has been developed from IAP9L-AGCM (Liang, 1996; Zeng and Mu, 2002; Zuo et al., 2004) at the Institute of Atmospheric Physics, Chinese Academy of Sciences. This model has been widely used to investigate present-day climate and paleoclimate (e.g., the mid-Holocene and the Last Glacial Maximum; Wang, 2002; Jiang et al., 2003; Jin et al., 2006; Ju et al., 2007; Zhang et al., 2007). Prior studies have reported that it shows good model performance, especially in the East Asia region (Lang et al., 2004; Ju and Lang, 2011). The new version (IAP4) has a horizontal grid resolution of $1.4^\circ \times 1.4^\circ$ with 26 vertical levels ranging from the surface to 10 hPa. Its higher resolution will be helpful to improve performances in simulating the large-scale summer climate in East Asia (Wang and Wang, 2013).

2.2. Experiment design

In an attempt to investigate the spatial pattern of summer rainfall in this RCM, a suite of simulations was carried out following the Paleoclimate Modelling Intercomparison Project (PMIP; <http://pmip.lsce.ipsl.fr/>) experiments using IAP4 and WRF. The details of the model settings are listed in Table 1. There were two groups of parallel simulations: present-day simulations (hereafter referred to as "0K"), and mid-Holocene simulations (hereafter referred to as "6K").

Table 1. Boundary conditions and model settings for the simulation.

Case name	Model name	Eccentricity	Obliquity ($^\circ$)	Angular precession ($^\circ$)	CO ₂ (ppm)	CH ₄ (ppb)	NO ₂ (ppb)	Boundary conditions	Simulation period (yr)
G0K	IAP4	0.016724	23.446	102.04	280	760	270	—	28
G6K	IAP4	0.018682	24.105	0.87	280	650	270	—	28
R0K	WRF	0.016724	23.446	102.04	280	760	270	G0K	13
R6K	WRF	0.018682	24.105	0.87	280	650	270	G6K	13

The differences between these two simulation groups included the orbital parameters (eccentricity, obliquity and angular precession) and greenhouse gas concentrations. The vegetation distribution was the same as that of the present day, and the SST dataset used was the prescribed climatological data (Otto-Bliesner et al., 2006); the SST in the mid-Holocene was cooler than that at present over the East China Sea. The IAP4 simulations for the present day (GCM-0K, G0K for short) and mid-Holocene (GCM-6K, G6k for short) provided the initial and boundary conditions for the corresponding WRF simulations [RCM-0K (R0k) and RCM-6K (R6K for short)].

The domain for the regional climate simulation covered mainland China and nearby regions, consisting of 164 longitude grids and 128 latitude grids, at a resolution of 50 km. The reason for such a large area was that WRF can achieve more freedom to develop its own mesoscale circulations (Ge et al., 2013; Yu, 2013). The model physics included the Lin et al. microphysics scheme (Lin et al., 1983), the Rapid Radiative Transfer Model (RRTM) longwave radiation scheme (Mlawer et al., 1997), the Dudhia shortwave radiation scheme (Dudhia, 1989), and the Noah land surface model (Chen and Dudhia, 2001).

In both the G0K and G6K simulations, IAP4 was run for 28 model years, with the last 13 model-year results driving the WRF simulations. All the model results presented in the following sections are averages from the last 12 years of present and mid-Holocene simulations. The performances of the model simulations were evaluated by spatial correlation coefficient (SCC), root-mean-square differences (RMSDs) and statistical significance calculated according to the Student's *t*-test at the 95% confidence level.

2.3. Model validation

Firstly, the performance of the present-day regional climate simulation was validated against observed temperature and precipitation for the period 1983–2002. The observations, including the gridded daily temperature (CN05, details

can be found in Xu et al., 2009) and precipitation (XIE, details can be found in Xie et al., 2007) data at $0.5^\circ \times 0.5^\circ$ resolution, provide a high-quality estimation of temperature and precipitation distribution over China up to the present day. Strictly speaking, the present-day simulations were actually the pre-industrial control simulations according to the boundary conditions and model settings following the PMIP experiments listed in Table 1, and the results should have been validated against the corresponding pre-industrial observations. However, considering the availability of observational data, we chose CN05 and XIE data to conduct the model validation.

Figure 1 shows the annual mean temperature and precipitation from observations, as well as the simulations from IAP4 and WRF. Regarding surface air temperature (Figs. 1a–c), we can see obvious latitudinal distribution characteristics from the observations; that is, the temperature is high in South China and low in North China. The Tibetan Plateau is an exception; this area contains the world's highest mountains and stores more snow and ice than anywhere in the world outside the polar regions, and the temperature is much lower than surrounding areas. Another distinct area is the Tarim Basin; this area contains the largest desert of China and the temperature is high. Compared to the observation, IAP4 can reasonably reproduce the main features of temperature; the temperature is higher in the south and lower in the north, and the simulation over the Tibetan Plateau and Tarim Basin also compares well with the observation. The SCC of simulation against observation was calculated to be as high as 0.92. Further, the WRF simulation shows significant improvement in terms of the geographical distribution; it captures many local characteristics due to topographical effects, such as the warmer center located in the Sichan Basin and the cold centers along the Tianshan Mountains. The SCC was calculated to be 0.97, which is much higher than for the IAP simulation. Compared to the WRF simulation, the simulation by IAP4 is much smoother, and thus shows little ability in capturing the topography-induced variation and local small-scale details.

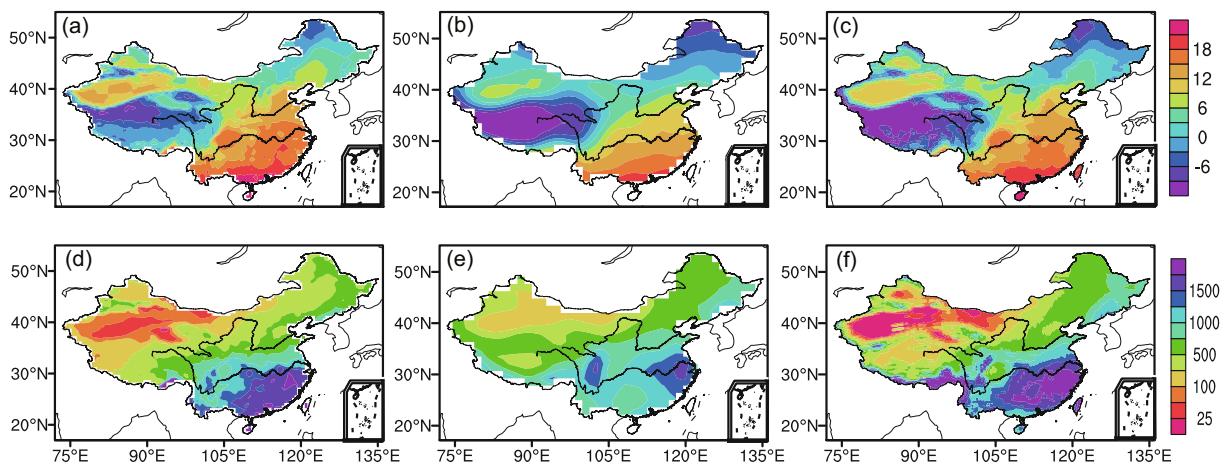


Fig. 1. Present-day annual mean temperature (upper panel; units: $^\circ\text{C}$) and precipitation (bottom panel; units: mm) from observations (a, d), IAP4 simulation (b, e), and WRF simulation (c, f).

Precipitation according to observations and the model simulation is present in Figs. 1d–f. The main characteristics of observed precipitation is the longitudinal heterogeneity; that is, China receives more precipitation over its southeast coastal regions but little precipitation over its northwest arid areas. The annual mean precipitation is more than 1500 mm in Southeast China, but less than 25 mm in the desert regions of Northwest China. IAP4 can reproduce the major rainfall patterns quite reasonably; the simulated precipitation amount is higher over East China and lower over Northeast China, and the SCC was calculated to be as high as 0.7. Compared to the IAP4 simulation, the WRF model obviously shows better performance. From Fig. 1f, we can see that WRF is able to reproduce the rainfall distribution more reasonably, especially for the wet center over Southeast China and the dry center over Northwest China. In addition, WRF can reproduce many of the orographic precipitation features due its high resolution. The SCC of the WRF simulation against the observation was calculated to be 0.78. The greatest improvement occurred in Southeast China. In the IAP4 simulation, the wet center locates over the lower reaches of the Yangtze River, which is in disagreement with the observation; this disagreement is quite common among GCMs. In the WRF simulation, the location is reasonable compared to the observation, and the simulated amount of precipitation also compares to the observation very well. Based on these comparison results, we can conclude that the precipitation simulated by WRF is more reliable, especially over Southeast China.

Figure 2 shows the Taylor diagram of temperature and precipitation. Taylor diagrams (Taylor, 2001) provide a way

of graphically summarizing how closely a pattern matches observations. From the figure, we can see that the spatial correlation of the WRF simulation against observation is higher than that of IAP4 for both temperature and precipitation, and the centered RMSD (distance to the point on the *x*-axis identified as “REF”) is lower in the WRF simulation in most of the cases.

Taken together, compared to IAP4, WRF shows better performance over China in terms of present-day climate simulation, including summer temperature and precipitation. The most obvious improvement is that WRF represents the local-scale dynamic processes better and more realistically, thus producing “added value” (Luca et al., 2013) over the lower resolution IAP4 simulation. The summer precipitation simulation from WRF is more reliable over eastern China, and thus it can be expected that WRF is also able to provide “added value” for precipitation change simulation over these regions.

3. Results

3.1. Changes in surface temperature

Proxy indicators from pollen, ice cores, lake cores and so on reveal that the climate was generally warmer in East Asia in the mid-Holocene (Wang et al., 2010, Fig. 5a; Jiang et al., 2012, Fig. 3d). Most of the records indicate prevailing warm conditions, with the annual mean temperature increasing by about 1 K in South China, by about 2 K in the Yangtze River valley region, by 3 K in most parts of northern China, and by 4–5 K on the Qinghai–Tibetan Plateau (Yao et al., 1991; Shi et al., 1993; Jiang et al., 2012). As for the summer/winter mean temperature change, there are still too few proxy data to form a spatial dataset to compare with the model result.

Figure 3 presents the differences in the simulated annual and seasonal mean surface temperature (6K minus 0K). Both IAP4 and WRF show lower annual air temperature in North, South and parts of West China during the mid-Holocene, and the lower annual air temperature is mainly caused by the lower winter air temperature since the summer air temperature is higher (warm summer and cold winter). The WRF-simulated annual temperature shows larger magnitude than that of IAP4 in North and West China. The average annual temperature change in mainland China is -0.42 (-0.41) K for IAP4 (WRF).

As for summer, the June–July–August (JJA) mean temperature increases almost all over China, with larger magnitude in the high-latitude regions and the Tibetan Plateau. In the margin regions of South China, the temperature change is not obvious. The average temperature change in mainland China is 1.29 (1.43) K for IAP4 (WRF). As for winter, the December–January–February (DJF) mean temperature decreases over most areas of China, which follows closely the solar radiation decline in the Northern Hemisphere (Jiang et al., 2012). The two model simulations, and a previous simulation using CCSM3 (Zhou and Zhao, 2009a) show strong agreement in terms of seasonal temperature change. How-

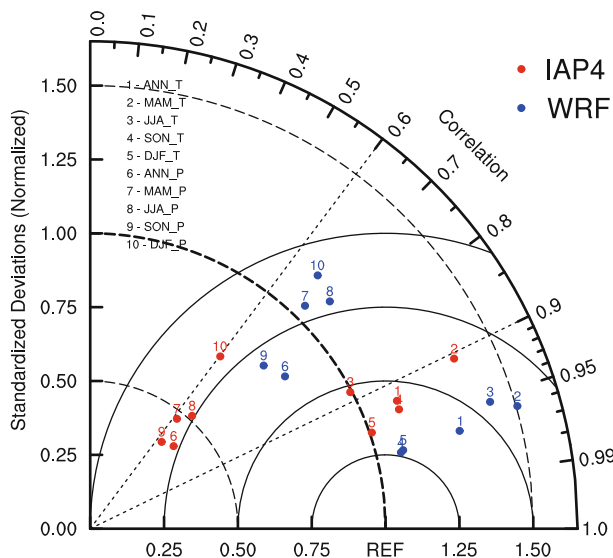


Fig. 2. Taylor diagram of temperature ($^{\circ}\text{C}$) and precipitation (mm d^{-1}) between the present-day simulation and observations over mainland China. The observational climatology was derived from the CN05 (Xu et al., 2009) and XIE (Xie et al., 2007) datasets for the period 1982–2002. T, temperature; P, precipitation; MAM, March–April–May; JJA, June–July–August; SON, September–October–November; DJF, December–January–February.

ever, it should be noted that considerable mismatch can be seen with respect to annual mean temperature between model simulations (both IAP4 and WRF) and proxies (Jiang et al., 2012, Fig. 3d). This mismatch, which is similar with results from most climate models participating in the current stage of PMIP, was carefully addressed in the study by Jiang et al. (2012). The model–data mismatch in annual mean temperature over China is an important issue in paleoclimate studies, and whether the inconsistency arises from the models, from the proxy data, or from both sides, is still unclear (Jiang et al., 2012).

3.2. Changes in precipitation

As mentioned above, proxy data from lake cores, ice cores and so on indicate the annual mean precipitation in-

creased over North China and decreased over the lower reaches of the Yangtze River valley in the mid-Holocene. Figure 4 shows the annual and seasonal mean precipitation change according to IAP4 and WRF. From Fig. 4a, we can see that, just as most GCMs did in the PMIP project, IAP4 shows an overall wetter condition over mainland China, especially in North China. In the regions of the lower reaches of the Yangtze River valley and Southeast China, the precipitation change is not obvious. On the contrary, the results of WRF agree much more closely with the proxy data. The magnitude of precipitation change in the WRF simulation is much larger; in the regions of the lower reaches of the Yangtze River valley, the precipitation decreases by about 20% in the WRF simulation. The improvement from WRF over this region is mainly due to summer precipitation change, as the

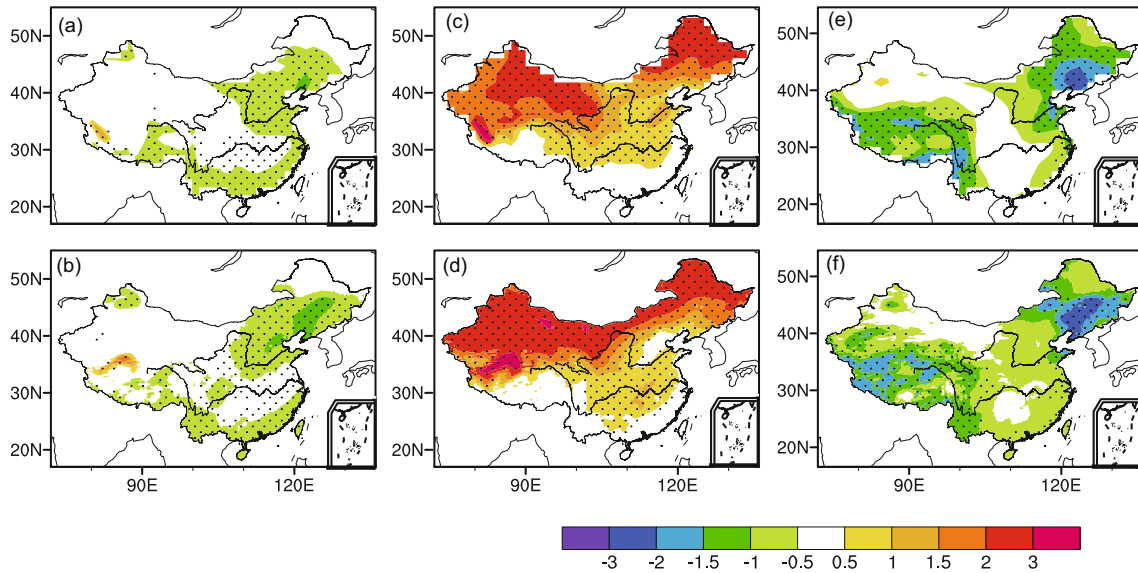


Fig. 3. (a, b) Annual mean, (c, d) JJA, and (e, f) DJF air temperature change (6K minus 0K; shading; units: °C) for IAP4 (upper panels) and WRF (lower panels). Areas with confidence levels greater than 95% are dotted.

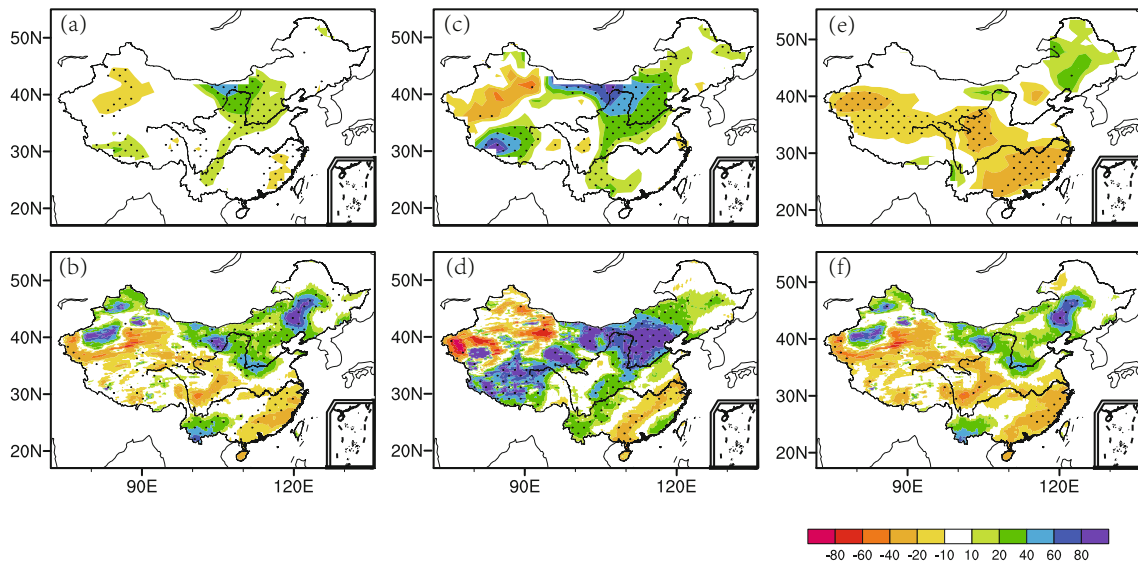


Fig. 4. (a, b) Annual mean, (c, d) JJA, and (e, f) DJF precipitation change (6K minus 0K; shading; units: %) for IAP4 (upper panels) and WRF (lower panels). Areas with confidence level greater than 95% are dotted.

difference of winter precipitation change between IAP4 and WRF is not obvious.

Figures 4c and d show the summer precipitation change from IAP4 and WRF. In the IAP4 simulation, the precipitation increases in North China, part of the Tibetan Plateau, and Southwest China; the strongest precipitation increase occurs in North China and mid-southern Tibet. The areas with less rainfall are located in Northwest China, covering the Tarim Basin and western Tibet. However, in the WRF simulation, the magnitude of precipitation is much larger, and the spatial pattern of precipitation change over the eastern part of China is different from the IAP4 simulation. The precipitation increases over Northeast China, Inner Mongolia, North China, Central China, Southwest China, and most parts of the Tibetan Plateau in the WRF simulation, but decreases over the lower reaches of the Yangtze River valley. This rainfall change pattern agrees better with the proxy data, and if taking the better performances of the WRF model in simulating the present-day climate in these areas into consideration, we can conclude with confidence that RCMs show better performances in terms of precipitation simulation.

For winter precipitation change, we can see that the precipitation decreases over northern parts of China but increases over southern parts. The main pattern of precipitation change from the WRF simulation is similar to that of IAP4, but with larger magnitude.

It should be mentioned that there also exists a mismatch between the model simulations and proxies. For example, proxy data indicate wetter conditions over the eastern Tibetan Plateau, while according to the models, the precipitation decreases over this region. This mismatch in precipitation also needs further investigation.

3.3. Changes in summer SST and monsoon circulation

As mentioned above, the better performance of the WRF model in simulating the annual mean precipitation change in the mid-Holocene is due to the improvement of summer rainfall simulation. In order to investigate the mechanism for summer rainfall change, we analyze the corresponding changes in surface wind, pressure, and SST, which is shown in Fig. 5. As the SST change is the same in IAP4 and WRF, we only show the SST data from IAP4, but for monsoon circulation analysis, we use both IAP4 and WRF results.

From Fig. 5a, we can see an apparent cool summer SST over the nearby oceans in the mid-Holocene; the SST decreases by 0.2 K–0.8 K, with large magnitude in the high latitudes. This cool summer SST is favorable for the enhancement of land–sea thermal contrast (He, 2013), thus enhancing the EASM, which can be found in Figs. 5c and d. From these two figures, we can see a negative (positive) anomaly in surface pressure in North China (East China Sea), and a strong southerly wind anomaly over East China in both the IAP4 and WRF simulation. This circulation anomaly can also be found in simulations by CCSM3 (Zhou and Zhao, 2009b), and is favorable for the enhancement of summer rainfall over North China (Fig. 4d). It has been revealed very well in monsoon studies using observation data that the enhanced EASM is

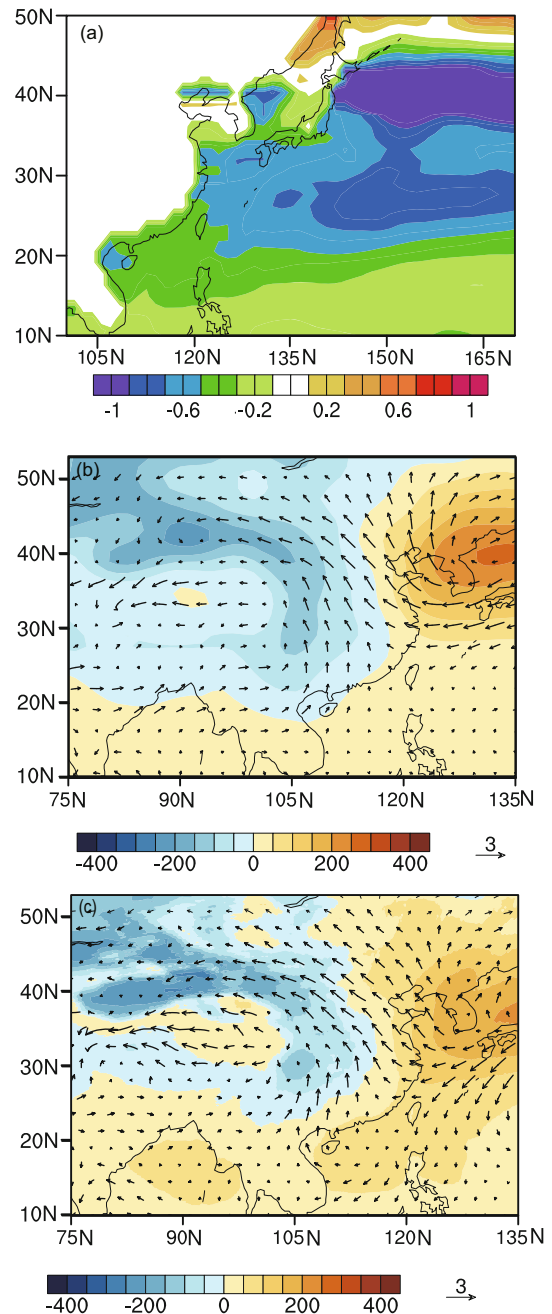


Fig. 5. (a) The SST (shading; units: K) change (6K minus 0K) in IAP4 shared with WRF and the JJA surface wind (streams; units: m s^{-1}) and surface pressure (shading; units: Pa) change (6k minus 0k) from IAP4 (b) and WRF (c).

related to the northward shift of the west Pacific subtropical high (Zhang et al., 2003; Zhu et al., 2010). This shift can correspondingly cause the summer rainfall to decrease over the lower reaches of the Yangtze River Basin (Zhang et al., 2003; Wang and Huang, 2006). From the above analysis, we can see that the summer SST and monsoon changes all indicate an SDNF rainfall pattern; this also explains the dynamical mechanism for the summer rainfall change.

Both large-scale and regional-scale forces shape regional climate change, so the reason why WRF can reproduce the

SDNF rainfall pattern may relate to small-scale precipitation change. More specifically, the precipitation decrease over the lower reaches of the Yangtze River valley may relate to small-scale precipitation change. In Fig. 6, the precipitation is divided into two parts based on the WRF model results: cumulus precipitation and small-scale precipitation, and the precipitation changes are the combination of these two parts. From the figure, we can see that, besides the cumulus precipitation change, the small-scale precipitation change is also quite important; the magnitude of precipitation change from these two parts is comparable. Although the cumulus precipitation change is also decreasing over the lower reaches of Yangtze River valley, the results presented in this figure certainly indicate that small-scale precipitation change is vital to regional precipitation change, and this small-scale precipitation change can be better represented in RCM simulations.

From previous studies we know that cold summer SSTs, enhanced summer EASM, and the summer SDNF pattern are dynamically related. Furthermore, besides the proxy data in Shanghai mentioned previously, other evidence based on SST and EASM proxy reconstructions also support the SDNF summer rainfall pattern (Marzin and Braconnot, 2009; Yokoyama et al., 2011; Jiang et al., 2013). The studies reveal that the northern South China Sea was cooler and the EASM was stronger than present during summer in the mid-Holocene. In other words, the proxy evidence for the mid-Holocene indicates the SDNF rainfall change pattern, which can be reproduced by the WRF simulation.

4. Summary and discussion

In this study, we investigated the main rainfall pattern according to state-of-the-art GCM and RCM simulations, and the results showed that, compared to IAP4, WRF shows better performance over China in terms of present-day surface air temperature and precipitation due to the improvements in the representation of local-scale dynamic processes. Summer rainfall simulation from WRF is more reliable over eastern China, and WRF can produce “added value” for precipitation change simulation over these regions.

The simulated annual mean temperature decrease in the

mid-Holocene and the “warm summer/cold winter” feature summarize the main characteristics of the simulated seasonal temperature change. The well-known model–data mismatch in annual temperature over China also exists in this simulation, but whether or not the inconsistency arises from the models, from the proxy data, or from both sides, is still unclear.

We have shown that the WRF reproduces the SDNF rainfall pattern in the mid-Holocene, while IAP4 fails to do so. The main reason for this is the improvement in summer climate simulation. Furthermore, the corresponding change of SST and EASM was analyzed to illustrate the reliability, and proxy evidence based on SST and the EASM also support the reliability of the WRF simulation. Besides, many recent studies have emphasized the importance of the thermal contrasts themselves (including the APO) and their influences on Asian monsoon and rainfall (Zhao et al., 2007, 2011, 2012; Sun et al., 2010; Chen et al., 2013), and thus further in-depth investigations regarding the mechanism of the rainfall change are required.

From the results of this study, we can see that there are also some mismatches between the simulations and proxy data, and thus the possible sources of the uncertainty should be addressed. Wang (1999) emphasized the important effects of vegetation and soil in 6k simulations, and his research indicated that considering the changes of vegetation and soil in simulations could further modulate monsoon precipitation. Moreover, atmosphere–ocean–land feedback mechanisms also play important roles in regulating mid-Holocene climate (Wang, 2002; Harrison et al., 2003; Tian and Jiang, 2013). Studies have revealed that ocean feedback mechanisms and the change of ENSO might also have affected climate (Liu et al., 2000, 2004). These kinds of feedback mechanisms may also affect RCM processes, and further simulation of climate change during the mid-Holocene should consider the effects of vegetation, soil and ocean feedback.

Model deficiencies can also explain model–proxy mismatches, not only in terms of RCMs, but GCMs as well. This is because the boundary conditions used for RCMs come from GCMs in the first place. Although RCMs can improve the ability of GCMs, the overall pattern is generally the same

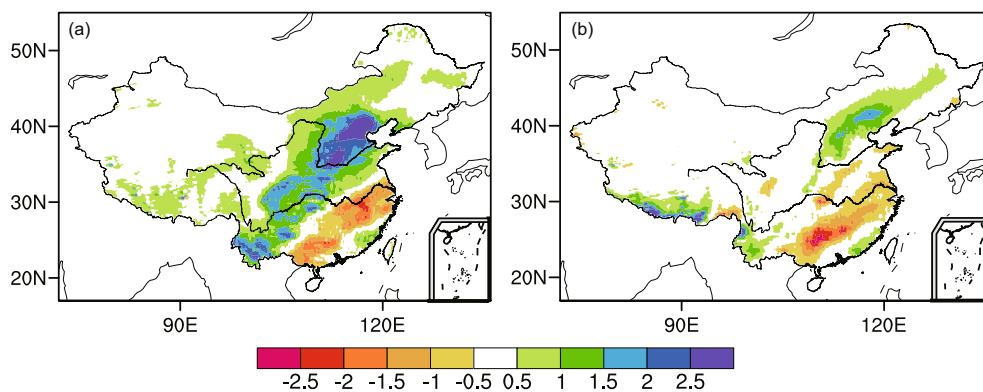


Fig. 6. The (a) cumulus precipitation change and (b) small-scale precipitation change in the WRF simulation. Units: mm d^{-1} .

as the GCM. Thus, GCM bias could help explain the model-proxy mismatches uncovered in the present study.

However, further research using atmosphere–ocean general circulation models (AOGCMs) is still needed. Since the fully coupled version of IAP4 (CAS ESM) is currently being developed, it is expected that this will be the main tool for future work of this kind. Another important component that should be taken into consideration is land surface change. Recent studies have revealed that land cover change in East Asia not only modifies the local climate, but also changes the climate in North Africa and the Middle East via teleconnections (Dallmeyer and Claussen, 2011). More experiments, including vegetation and soil dynamics, should be carried out to better understand mid-Holocene climate change over China.

Acknowledgements. This research was jointly supported by the “Strategic Priority Research Program” of the Chinese Academy of Sciences (Grant XDB03020602), the National Natural Science Foundation of China (Grant No. 41130103), the “Strategic Priority Research Program” of the Chinese Academy of Sciences (Grant No. XDA05120703), and the “Introduction of Advanced International Forestry Science and Technology” of the State Forestry Administration (2012-4-79).

REFERENCES

- Berger, A. L., 1978: Long-term variations of daily insolation and Quaternary climatic changes. *J. Atmos. Sci.*, **35**, 2362–2367.
- Braconnot, P., and Coauthors, 2007: Results of PMIP2 coupled simulations of the mid-Holocene and Last Glacial Maximum-part 1: Experiments and large-scale features. *Climate of the Past*, **3**, 261–277.
- Brown, J., M. Collins, A. W. Tudhope, and T. Toniazzo, 2008: Modelling mid-Holocene tropical climate and ENSO variability: towards constraining predictions of future change with palaeo-data. *Climate Dyn.*, **30**, 19–36.
- Cai, Y. L., Z. Y. Chen, W. Zhang, Z. Y. Guo, and Y. Chen, 2001: Climate fluctuation of the western Shanghai District by correspondence analysis since 8.5 kaB.P. *Journal of Lake Sciences*, **13**, 118–126. (in Chinese)
- Chang, C-P., Y. S. Zhang, and T. Li, 2000: Interannual and interdecadal variations of the East Asian summer monsoon and tropical Pacific SSTs. Part I: Roles of the subtropical ridge. *J. Climate*, **13**, 4326–4340.
- Chen, F., and J. Dudhia, 2001: Coupling an advanced land surface hydrology model with the Penn State-NCAR MM5 modeling system. Part I: Model implementation and sensitivity. *Mon. Wea. Rev.*, **129**, 569–585.
- Chen, H. P., J. Q. Sun, and X. L. Chen, 2012: The projection and uncertainty analysis of summer precipitation in China and the variations of associated atmospheric circulation field. *Climatic and Environmental Research*, **17**, 171–183. (in Chinese)
- Chen, X. L., T. J. Zhou, and L. W. Zou, 2013: Variation characteristics of the Asian-Pacific Oscillation in boreal summer as simulated by the LASG/IAP climate system model FGOALS-gl. *Acta Meteorologica Sinica*, **71**, 23–37 (in Chinese).
- Dallmeyer, A., and M. Claussen, 2011: The influence of land cover change in the Asian monsoon region on present-day and mid-Holocene climate. *Biogeosciences*, **8**, 1499–1519.
- Diffenbaugh, N. S., and L. C. Sloan, 2004: Mid-Holocene orbital forcing of regional-scale climate: A case study of western North America using a high-resolution RCM. *J. Climate*, **17**, 2927–2937.
- Ding, Y. H., Z. Y. Wang, and Y. Sun, 2008: Inter-decadal variation of the summer precipitation in East China and its association with decreasing Asian summer monsoon. Part I: Observed evidences. *Int. J. Climatol.*, **28**, 1139–1161.
- Dudhia, J., 1989: Numerical study of convection observed during the winter monsoon experiment using a mesoscale two-dimensional model. *J. Atmos. Sci.*, **46**, 3077–3107.
- Fu, J. J., S. L. Li, and D. H. Luo, 2009: Impact of global SST on decadal shift of East Asian summer climate. *Adv. Atmos. Sci.*, **26**, 192–201, doi: 10.1007/s00376-009-0192-z.
- Gao, X. J., J. S. Pal, and F. Giorgi, 2006: Projected changes in mean and extreme precipitation over the Mediterranean region from a high resolution double nested RCM simulation. *Geophys. Res. Lett.*, **33**, L03706, doi: 10.1029/2005GL024954.
- Gao, X. J., Y. Shi, and F. Giorgi, 2011: A high resolution simulation of climate change over China. *Science China: Earth Sciences*, **54**, 462–472.
- Ge, Q. S., X. Z. Zhang, and J. Y. Zheng, 2013: Simulated effects of vegetation increase/decrease on temperature changes from 1982 to 2000 across the Eastern China. *Int. J. Climatol.*, doi:10.1002/joc.3677. (in Press)
- Hargreaves, J. C., and J. D. Annan, 2009: On the importance of paleoclimate modelling for improving predictions of future climate change. *Clim. Past*, **5**, 803–814.
- Harrison, S. P., J. E. Kutzbach, Z. Liu, P. J. Bartlein, B. Otto-Bliessner, D. Muhs, I. C. Prentice, and R. S. Thompson, 2003: Mid-Holocene climates of the Americas: a dynamical response to changed seasonality. *Climate Dyn.*, **20**, 663–688.
- Hawkins, E., and R. Sutton, 2011: The potential to narrow uncertainty in projections of regional precipitation change. *Climate Dyn.*, **37**, 407–418.
- He, S. P., 2013: Reduction of the East Asian winter monsoon interannual variability after the mid-1980s and possible cause. *Chinese Science Bulletin*, **58**, 1331–1338.
- Jiang, D. B., H. J. Wang, D. Helge, and X. M. Lang, 2003: Last glacial maximum over China: Sensitivities of climate to paleovegetation and Tibetan ice sheet. *J. Geophys. Res.*, **108**, 4102, doi: 10.1029/2002JD002167.
- Jiang, D. B., X. M. Lang, Z. P. Tian, and T. Wang, 2012: Considerable model-data mismatch in temperature over China during the Mid-Holocene: Results of PMIP simulations. *J. Climate*, **25**, 4135–4153.
- Jiang, D. B., X. M. Lang, Z. P. Tian, and L. X. Ju, 2013: Mid-Holocene East Asian summer monsoon strengthening: Insights from Paleoclimate Modeling Intercomparison Project (PMIP) simulations. *Palaeogeography, Palaeoclimatology, Palaeoecology*, **369**, 422–429.
- Jin, L. Y., H. J. Wang, F. H. Chen, and D. B. Jiang, 2006: A possible impact of cooling over the Tibetan Plateau on the mid-Holocene East Asian monsoon climate. *Adv. Atmos. Sci.*, **23**, 543–550, doi: 10.1007/s00376-006-0543-y.
- Ju, L. X., and X. M. Lang, 2011: Hindcast experiment of extraseasonal short-term summer climate prediction over China with RegCM3.IAP9L-AGCM. *Acta Meteorologica Sinica*, **25**, 376–385.

- Ju, L. X., H. J. Wang, and D. B. Jiang, 2007: Simulation of the Last Glacial Maximum climate over East Asia with a regional climate model nested in a general circulation model. *Palaeogeography, Palaeoclimatology, Palaeoecology*, **248**, 376–390.
- Knutti, R., and J. Sedlacek, 2012: Robustness and uncertainties in the new CMIP5 climate model projections. *Nature Climate Change*, **3**, 369–373, doi: 10.1038/NCLIMATE1716.
- Kutzbach, J. E., and Z. Liu, 1997: Response of the African monsoon to orbital forcing and ocean feedbacks in the middle Holocene. *Science*, **278**, 440–443.
- Lang, X. M., H. J. Wang, and D. B. Jiang, 2004: Extraseasonal short-term predictions of summer climate with IAP9L-AGCM. *Chinese Journal of Geophysics*, **47**, 19–24.
- Liang, X. Z., 1996: Description of a nine-level grid point atmospheric general circulation model. *Adv. Atmos. Sci.*, **13**, 269–298.
- Lin, Y. L., R. D. Farley, and H. D. Orville, 1983: Bulk parameterization of the snow field in a cloud model. *J. Appl. Meteor. Climatol.*, **22**, 1065–1092.
- Liu, G., P. Zhao, and J. M. Chen, 2011: A 150-year reconstructed summer Asian-Pacific Oscillation index and its association with precipitation over eastern China. *Theor. Appl. Clim.*, **103**, 239–248.
- Liu, Z., J. Kutzbach, and L. X. Wu, 2000: Modeling climate shift of El Niño variability in the Holocene. *Geophys. Res. Lett.*, **27**, 2265–2268.
- Liu, Z., S. P. Harrison, J. Kutzbach, and B. Otto-Bliesner, 2004: Global monsoons in the mid-Holocene and oceanic feedback. *Climate Dyn.*, **22**, 157–182.
- Luca, A. D., R. de Elia, and R. Laprise, 2013: Potential for small scale added value of RCM's downscaled climate change signal. *Climate Dyn.*, **40**, 601–618.
- Marzin, C., and P. Braconnot, 2009: The role of the ocean feedback on Asian and African monsoon variations at 6 kyr and 9.5 kyr BP. *Comptes Rendus Geoscience*, **341**, 643–655.
- Mlawer, E. J., S. J. Taubman, P. D. Brown, M. J. Iacono, and S. A. Clough, 1997: Radiative transfer for inhomogeneous atmospheres: RRTM, a validated correlated-k model for the longwave. *J. Geophys. Res.*, **102**, 16 663–16 682, doi: 10.1029/97JD00237.
- Otto-Bliesner, B. L., E. C. Brady, G. Clauzet, R. Tomas, S. Levis, and Z. Kothavala, 2006: Last glacial maximum and Holocene climate in CCSM3. *J. Climate*, **19**, 2526–2544.
- Shi, Y. F., and Coauthors, 1993: Mid-Holocene climates and environments in China. *Global and Planetary Change*, **7**, 219–233.
- Skamarock, W. C., and Coauthors, 2008: A description of the Advanced Research WRF version 3. Tech. Rep. NCAR/TN475+STR, National Center for Atmospheric Research, Boulder Co., 1–125.
- Sun, H. C., G. Q. Zhou, and Q. C. Zeng, 2012: Assessments of the climate system model (CAS-ESM-C) using IAP AGCM4 as its atmospheric component. *Chinese J. Atmos. Sci.*, **36**, 215–233.
- Sun, J. Q., and H. J. Wang, 2012: Changes of the connection between the summer North Atlantic Oscillation and the East Asian summer rainfall. *J. Geophys. Res.*, **117**, D08110, doi: 10.1029/2012JD017482.
- Sun, Y., Y. H. Ding, and A. G. Dai, 2010: Changing links between South Asian summer monsoon circulation and tropospheric land-sea thermal contrasts under a warming scenario. *Geophys. Res. Lett.*, **37**, L02704, doi: 10.1029/2009GL041662.
- Taylor, K. E., 2001: Summarizing multiple aspects of model performance in a single diagram. *J. Geophys. Res.*, **106**, 7183–7192.
- Tian, Z. P., and D. B. Jiang, 2013: Mid-holocene ocean and vegetation feedbacks over East Asia. *Clim. Past*, **9**, 2153–2171.
- Wang, H. J., 1999: Role of vegetation and soil in the Holocene megathermal climate over China. *J. Geophys. Res.*, **104**, 9361–9367.
- Wang, H. J., 2000a: The interannual variability of the East Asian Monsoon and its relationship with SST in a coupled Atmosphere-Ocean-Land climate model. *Adv. Atmos. Sci.*, **17**, 31–47.
- Wang, H. J., 2000b: The seasonal climate and low frequency oscillation in the simulated mid-Holocene megathermal climate. *Adv. Atmos. Sci.*, **17**, 445–457.
- Wang, H. J., 2001: The weakening of the Asian monsoon circulation after the end of 1970's. *Adv. Atmos. Sci.*, **18**, 376–386.
- Wang, H. J., 2002: The mid-Holocene climate simulated by a grid-point AGCM coupled with a biome model. *Adv. Atmos. Sci.*, **19**, 205–218.
- Wang, S. W. and J. B. Huang, 2006: The relationship between flood/drought and Chinese ancient civilization in mid-Holocene. *Progress in Natural Science*, **16**, 1238–1244. (in Chinese)
- Wang, T., and H. J. Wang, 2013: Mid-Holocene Asian summer climate and its responses to cold ocean surface simulated in the PMIP2 OAGCMs experiments. *J. Geophys. Res.*, **118**, doi: 10.1029/2012JD018845.
- Wang, T., H. J. Wang, and D. B. Jiang, 2010: Mid-Holocene East Asian summer climate as simulated by the PMIP2 models. *Palaeogeography, Palaeoclimatology, Palaeoecology*, **288**, 93–102.
- Wicker, L. J., and W. C. Skamarock, 2002: Time splitting methods for elastic models using forward time schemes. *Mon. Wea. Rev.*, **130**, 2088–2097.
- Xie, P. P., A. Yatagai, M. Y. Chen, T. Hayasaka, Y. Fukushima, C. M. Liu, and S. Yang, 2007: A gauge-based analysis of daily precipitation over East Asia. *J. Hydrometeorol.*, **8**, 607–626.
- Xu, Y., X. J. Gao, Y. Shen, C. H. Xu, Y. Shi, and F. Giorgi, 2009: A daily temperature dataset over China and its application in validating a RCM simulation. *Adv. Atmos. Sci.*, **26**, 763–772, doi: 10.1007/s00376-009-9029-z.
- Yao, T. D., Z. C. Xie, X. L. Wu, and L. G. Thompson, 1991: Climatic-change since little ice-age recorded by Dunde ice cap. *Science in China Series B*, **34**, 760–767.
- Yokoyama, Y., A. Suzuki, F. Siringan, Y. Maeda, A. Abe-Ouchi, R. Ohgaito, H. Kawahata, and H. Matsuzaki, 2011: Mid-Holocene palaeoceanography of the northern South China Sea using coupled fossil-modern coral and atmosphere-ocean GCM model. *Geophys. Res. Lett.*, **38**, D20109, doi: 10.1029/2010GL044231.
- Yu, E. T., 2013: High-resolution seasonal snowfall simulation over Northeast China. *Chinese Science Bulletin*, **58**, 1412–1419, doi: 10.1007/s11434-012-5561-9.
- Yu, E. T., H. J. Wang, and J. Q. Sun, 2010: A quick report on a dynamical downscaling simulation over China using the nested model. *Atmos. Oceanic Sci. Lett.*, **3**, 325–329.
- Yu, E. T., H. J. Wang, J. Q. Sun, and Y. Q. Gao, 2012: Climatic response to changes in vegetation in the Northwest Hetao Plain as simulated by the WRF model. *Int. J. Climatol.*, **33**, 1470–1481.

- Zeng, Q. C., and M. Mu, 2002: On the design of compact and internally consistent model of climate system dynamics. *Chinese J. Atmos. Sci.*, **26**, 107–113.
- Zhang, R., D. B. Jiang, X. D. Liu, and Z. P. Tian, 2012: Modeling the climate effects of different subregional uplifts within the Himalaya-Tibetan Plateau on Asian summer monsoon evolution. *Chinese Science Bulletin*, **57**, 4617–4626.
- Zhang, Q. Y., S. Y. Tao, and L. T. Chen, 2003: The inter-annual variability of East Asian summer monsoon indices and its association with the pattern of general circulation over East Asia. *Acta Meteorologica Sinica*, **61**, 559–568. (in Chinese)
- Zhang, Y., and J. Q. Sun, 2012: Model projections of precipitation minus evaporation in China. *Acta Meteorologica Sinica*, **26**, 376–388.
- Zhang, Z. S., H. J. Wang, Z. T. Guo and D. B. Jiang, 2007: What triggers the transition of palaeoenvironmental patterns in China, the Tibetan Plateau uplift or the Paratethys Sea retreat? *Palaeogeography, Palaeoclimatology, Palaeoecology*, **245**, 317–331.
- Zhao, P., Y. N. Zhu, and R. H. Zhang, 2007: An Asia-Pacific teleconnection in summer tropospheric temperature and associated Asian climate variability. *Climate Dyn.*, **29**, 293–303.
- Zhao, P., S. Yang, and R. C. Yu, 2010: Long-term changes in rainfall over Eastern China and large-scale atmospheric circulation associated with recent global warming. *J. Climate*, **23**, 1544–1562.
- Zhao, P., S. Yang, H. J. Wang, and Q. Zhang, 2011: Interdecadal Relationships between the Asian-Pacific Oscillation and Summer Climate Anomalies over Asia, North Pacific and North America during Recent 100 Years. *J. Climate*, **24**, 4793–4799.
- Zhao, P., B. Wang, and X. J. Zhou, 2012: Boreal summer continental monsoon rainfall and hydroclimate anomalies associated with the Asian-Pacific Oscillation. *Climate Dyn.*, **39**: 1197–1207.
- Zhou, B. T., and P. Zhao, 2009a: Inverse correlation between ancient winter and summer monsoons in East Asia? *Chinese Science Bulletin*, **54**, 3760–3767.
- Zhou, B. T., and P. Zhao, 2009b: Coupled simulation result of seasonal evolution of southwesterly wind climate over eastern China in mid-Holocene. *Quaternary Sciences*, **29**, 211–220. (in Chinese)
- Zhou, B. T., and P. Zhao, 2010: Modeling variations of summer upper tropospheric temperature and associated climate over the Asian Pacific region during the mid-Holocene. *J. Geophys. Res.*, **115**, D20109, doi: 10.1029/2010JD014029.
- Zhou, B. T., and D. D. Xia, 2012: Interdecadal change of the connection between winter North Pacific Oscillation and summer precipitation in the Huaihe River valley. *Science China Earth Sciences*, **55**, 2049–2057.
- Zhou, X. J., P. Zhao, G. Liu, and T. J. Zhou, 2011: Characteristics of decadal-centennial-scale changes in East Asian summer monsoon circulation and precipitation during the Medieval Warm Period, Little Ice Age and in the present day. *Chinese Science Bulletin*, **56**(28–29), 3003–3011.
- Zhu, Y. L., H. J. Wang, W. Zhou, and J. H. Ma, 2010: Recent changes in the summer precipitation pattern in East China and the background circulation. *Climate Dyn.*, **36**, 1463–1473.
- Zuo, R. T., M. Zhang, D. L. Zhang, A. H. Wang, and Q. C. Zeng, 2004: Designing and climatic numerical modeling of 21-Level AGCM (IAP AGCM-III) Part I. dynamical framework. *Chinese J. Atmos. Sci.*, **28**, 659–673. (in Chinese)